Texture Classification Using Rotation Invariant LBP Based on Digital Polygons

Juan Pardo-Balado[1], Antonio Fernández[1(✉)], and Francesco Bianconi[2]

[1] Universidade de Vigo, School of Industrial Engineering,
Campus Universitario, Rúa Maxwell s/n, 36310 Vigo, Spain
jpardo@alumnos.uvigo.es, antfdez@uvigo.es
[2] Department of Engineering, Università degli Studi di Perugia,
Via G. Duranti, 93, 06125 Perugia, Italy
bianco@ieee.org

Abstract. This paper investigates the use of digital polygons as a replacement for circular interpolated neighbourhoods for extracting texture features through Local Binary Patterns. The use of digital polygons has two main advantages: reduces the computational cost, and avoids the high-frequency loss resulting from pixel interpolation. The solution proposed in this work employs a sub-sampling scheme over Andres' digital circles. The effectiveness of the method was evaluated in a supervised texture classification experiment over eight different datasets. The results showed that digital polygons outperformed interpolated circular neighbourhoods in most cases.

Keywords: Local Binary Patterns · Texture classification · Digital circles · Digital polygons · Rotation invariance

1 Introduction

Texture analysis plays a pivotal role in many machine vision applications including, among many others, material recognition, surface inspection and grading, remote sensing, computer-assisted diagnosis and content-based image retrieval. No surprise, then, that texture analysis has been attracting increasing research interest over the last four decades, and that many texture descriptors have appeared in the literature [14]. Among them, Local Binary Patterns (LBP) has emerged as one of the most successful methods due to the high descriptive capability, ease of implementation and low computational cost. In many applications it is mandatory that texture description be invariant to image rotation, for real world textures can occur at any orientation. In the case of LBP the usual way to achieve robustness against rotation consists of using circular neighbourhoods and grouping together all the binary patterns that can be transformed into each other through a discrete rotation around the central pixel. Since exact circular neighbourhoods are not possible on the square lattice of digital images, the common solution involves estimating the intensities of the points that do not

V. Murino et al. (Eds.): ICIAP 2015 Workshops, LNCS 9281, pp. 87–94, 2015.
DOI: 10.1007/978-3-319-23222-5_11

coincide with image pixels through bilinear interpolation [8]. Yet this approach has two main drawbacks: on the one hand, interpolation is time-consuming hence impractical in those applications where real-time processing is required; on the other, it is well-known that interpolation smooths the image and therefore alters the high-frequency content of the original signal producing artifacts and/or significant loss of information [4]. In this paper we propose a solution to overcome these problems. Our approach consists of replacing the interpolated circular neighbourhood by digital polygons. The vertices of the polygons perfectly overlap the image's pixels making interpolation unnecessary. To ensure robustness against rotation, the resemblance of digital polygons to the approximated circle is measured through one quantitative index, namely the circularity. From a set of image classification experiments we conclude that LBP features based on digital polygons are at least as good (and in general better) at discriminating textures than those based on the traditional circular neighbourhoods.

The remainder of the paper is organized as follows. After a brief review of the relevant literature we introduce the proposed method in Sec. 2, and describe the experimental set-up in Sec. 3. We summarise and discuss the results in Sec. 4, then conclude the paper with some final considerations and ideas for future research (Sec. 5).

2 Methodology

The problem of approximating circles on square lattices has long been a relevant topic in digital geometry and computer graphics, and studies on this subject can be traced as far back as to Gauss [7, Sec. 2.3.1]. The Bresenham's algorithm is one of the most common approaches to trace circles on raster devices, and has also been applied to image processing tasks such as circle extraction using Hough transform [13]. It can be shown that Bresenham's algorithm is the solution to the minimum residual distance displacement approximation problem for integer radius [9]. More recently, Andres' circles [1] were used to compute rotation invariant texture features from grey level co-occurrence matrices [2,12]. In the general form an Andres' circle of radius R and center $C \equiv (x_C, y_C) \in \mathbb{Z}^2$ is defined as follows:

$$\mathcal{C}_R = \{(x, y) \in \mathbb{Z}^2 \mid R - \frac{1}{2} \leq \sqrt{(x - x_C)^2 + (y - y_C)^2} < R + \frac{1}{2}\} \qquad (1)$$

Compared with Bresenham's a potential advantage of Andres' circles is that for a given center any pixel of the plane belongs to one and only one Andres' circle, a property which does not hold for Bresenham's. This is the reason why the approach presented herein is based on Andres' solution. In either case both Bresenham's and Andres' methods are unsuitable for computing rotation invariant LBP texture features since the number of pixels of the resulting circular neighbourhood grows rapidly as the radius of the digital circle increases, therefore producing excessively long feature vectors. To avoid this issue we propose a

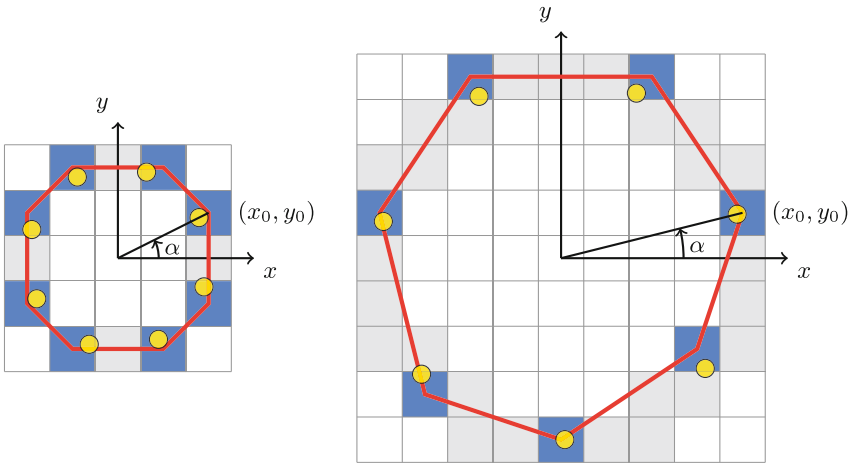

(a) $R = 2$ and $N = 8$ (b) $R = 4$ and $N = 7$

Fig. 1. Examples of digital polygons $\mathcal{P}_{R,N}$ of different number of vertices (N) obtained from digital circles of different radii (R). Shaded squares represent the pixels that make up Andres' circles. A subset of this set of pixels (shown in blue) are used as vertices of the polygons. The yellow dots depict the coordinates that Eq. 2 would yield if we removed the function $\|\cdot\|$ from the formulas.

sub-sampling scheme which retains a subset of N pixels of Andres' circle. This way we approximate the digital circle $\mathcal{C}_R$ trough a digital polygon $\mathcal{P}_{R,N}$ of N vertices, where $\mathcal{P}_{R,N} = \{(x_n, y_n) \in \mathbb{Z}^2 \mid n = 0, 1, \ldots N-1\} \subseteq \mathcal{C}_R$. The construction of such a digital polygon is summarised in Fig. 1. As a first step we select a starting pixel $(x_0, y_0) \in \mathcal{C}_R$ which represents the starting vertex of the polygon. Note that, in principle, any pixel of the Andres' circle could be chosen as the starting vertex, but, due to symmetry reasons, we can conveniently limit the choice to just one octant of the digital circle, i.e.: we assume $0 \leq \alpha \leq \pi/4$, where α is the counter-clockwise angle formed by the radius through the point (x_0, y_0) and the horizontal axis x. The coordinates of the remaining vertices are calculated through the following formulas:

$$\begin{aligned} x_n &= x_C + \|R\cos(2\pi n/N + \alpha)\| \\ y_n &= y_C + \|R\sin(2\pi n/N + \alpha)\| \end{aligned} \tag{2}$$

where $\|\cdot\|$ stands for the 'nearest integer'. If the decimal part of the argument of the function $\|\cdot\|$ is exactly 1/2 the returned value is the integer number farthest away from zero. Ideally the digital polygon should resemble a circle as closely as possible. As measure of the goodness-of-fit we consider the concept of *circularity*, also known as roundness or isoperimetric quotient [3]:

$$f_{\text{circ}} = \frac{4\pi A}{P^2} \tag{3}$$

where A and P denote the area and the perimeter of the digital polygon, respectively. The circularity of a circle is 1, whereas for any other shape is less than 1. Among the possible pixels that can be chosen as the starting vertex of the approximating polygon, we select the one that gives the highest circularity; when there is more than one solution we select the pixel with lowest α.

3 Experiments

To validate the proposed approach we performed a set of supervised texture classification experiments using rotation-invariant local binary patterns (LBP^{ri}) as texture features. For comparison purposes, rotation invariant LBP features were computed using the proposed digital polygons as well as the traditional circular neighbourhood. In the second case the intensities of those neighbourhood points that do not coincide with image pixels were estimated through bilinear interpolation as recommended in [8]. We tested both methods over eight datasets (Tab. 1) derived from publicly available texture databases: ALOT, Brodatz, HeLa 2D, Kylberg-Sintorn, MondialMarmi, Outex 00045, Pap Smear and Vectorial (see Refs. [6,11] for further details). The resulting benchmark includes a large number of images and a broad variety of textures. In order to determine the influence of the radius of the digital circle and the number of vertices of the polygon we considered all possible pairs of whole numbers $(R, N) \in [1, 7] \times [5, 16]$ that are compatible with the existence of a digital polygon of the type described in Sec. 2. The circularity values of the considered polygons are shown in Table 2. The reader will notice that some of the cells of the table are empty. This is due to the following reasons: 1) the number of vertices of the approximating polygon cannot exceed the number of pixels of Andres' circle (for instance a polygon approximating a digital circle of radius $R = 2$ cannot have more than $N = 12$ vertices); 2) for some pairs of values, such as $R = 3$ and $N = 15$, Eq. 2 returns pixels coordinates that do not belong to the Andres' circle.

Table 1. Datasets used in the experiments: summary table

Dataset	No. of classes	No. of samples per class	Rotation angles
ALOT	80	16	0°, 60°, 120°, 180°
Brodatz	13	16	0°, 10°, 20°, 30°, 40°, 50°, 60°, 70°, 80°, 90°
HeLa 2D	10	20	N/A
Kylberg-Sintorn	25	16	0°, 40°, 80°, 120°, 160°, 200°, 240°, 280°, 320°
MondialMarmi	12	16	0°, 5°, 10°, 15°, 30°, 45°, 60°, 75°, 90°
Outex 00045	45	20	0°, 5°, 10°, 15°, 30°, 45°, 60°, 75°, 90°
Pap Smear	2	204	N/A
Vectorial	20	16	0°, 10°, 20°, 30°, 40°, 50°, 60°, 70°, 80°, 90°

Table 2. Circularity (in percentage) as a function of N and R. Number of features indicates the dimension of the $\mathrm{LBP}^{ri}_{N,R}$ histogram.

Number of vertices	Number of features	Radius						
		1	2	3	4	5	6	7
5	8	80.85	84.41	85.82	86.00	86.19	86.45	86.41
6	14	80.85	90.00	90.00	90.64	90.41	90.64	90.64
7	20	80.01	90.00	92.26	92.53	93.00	92.87	93.10
8	36	78.54	94.33	94.33	94.25	94.79	94.36	94.79
9	60	–	92.34	94.43	94.37	–	95.25	95.60
10	108	–	94.33	94.43	95.90	96.15	96.26	96.49
11	188	–	94.33	94.41	95.22	96.51	96.63	96.80
12	352	–	94.33	94.33	97.50	96.61	97.50	97.48
13	632	–	–	94.41	93.75	96.74	96.53	97.41
14	1182	–	–	94.33	96.68	96.61	96.24	97.99
15	2192	–	–	–	95.62	–	96.32	97.61
16	4116	–	–	94.33	95.90	98.50	98.06	98.50

The texture samples were classified using a nearest-neighbourhood (1-NN) classifier with Euclidean distance. It is reasonable to expect that classifiers such as SVM or SOM might perform better. However, we avoided such classifiers owing to the fact their performance strongly depends on a number of parameters which are notoriously difficult to determine [5]. The overall accuracy was estimated through split-half validation with stratified sampling: in each classification problem each dataset was randomly subdivided into two equal parts (train and test set) in which the proportion of samples of each class was the same as in the whole dataset. For each problem the accuracy was estimated as the proportion of samples of the test set classified correctly. In each dataset the process was repeated for all the rotation angles available in that dataset in the following way: the train samples were always picked from the unrotated textures (images taken at $0°$), while the test samples were taken from textures rotated by θ_k degrees, $k \in \{0, \ldots, K-1\}$ where K is the number of rotation angles provided by that dataset (see Tab.1). The accuracy was the average of the classification rates obtained for each rotation angle. For a stable estimation the classification accuracy was averaged over 100 random partitions of the database into train and test set.

4 Results and Discussion

The main effects on the overall classification accuracy resulting from using digital polygons or interpolated circular neighbourhoods are summarised in Tab. 3. For each dataset and rotation angle the table reports the classification accuracy averaged over all the combinations of (N, R) considered in the experiments (see Tab. 2). The figures show that, on average, digital polygons outperformed interpolated circles (the reverse occurred with the Brodatz dataset only). To validate these findings a statistical test (Student's t-test, significance level 5%) was also performed on each combination of (N, R) to determine whether the difference

Table 3. Average classification accuracy obtained using digital polygons (p) and interpolated circular neighbourhoods (c).

	Dataset											
	ALOT		Brodatz		Kylberg-Sintorn		Mondial Marmi		Outex 00045		Vectorial	
Angle	p	c	p	c	p	c	p	c	p	c	p	c
0°	74.8	67.4	97.4	97.2	99.2	98.8	81.9	81.1	72.1	65.5	85.3	85.0
5°							81.8	80.4	72.2	65.7		
10°			90.1	89.5			81.8	80.9	72.0	65.1	78.0	77.3
15°							82.0	80.8	71.8	64.7		
20°			87.1	88.2							79.6	78.0
30°			88.1	90.1			80.5	80.3	72.9	65.8	80.0	78.3
40°			87.9	89.6	88.1	86.2					80.1	77.8
45°							81.6	81.7	72.7	65.8		
50°			87.7	90.2							80.0	77.9
60°	72.4	65.7	88.0	90.4			82.7	83.2	71.8	65.1	81.4	79.5
70°			87.7	90.3							80.5	79.1
75°							84.2	84.7	70.7	64.3		
80°			86.7	88.8	87.5	85.8					79.0	78.3
90°			88.9	89.1			85.5	86.1	70.4	64.1	87.2	86.7
120°	69.7	63.1			89.6	88.3						
160°					91.0	88.8						
180°	72.7	65.3										
200°					92.0	90.2						
240°					91.8	90.6						
280°					82.8	80.6						
320°					89.7	87.8						
Avg	**72.4**	65.4	89.0	**90.3**	**90.2**	88.6	**82.4**	82.1	**71.8**	65.1	**81.1**	79.8
Std	2.1	**1.8**	3.1	**2.5**	**4.4**	4.9	**1.5**	2.1	0.8	**0.6**	**2.9**	3.3

	Dataset			
	HeLa 2D		Pap Smear	
Angle	p	c	p	c
N/A	**54.3**	53.9	**72.8**	72.3

between the performance of the two methods was statistically significant. The outcome of this analysis is summarised in Fig. 2. For each combination the figure reports the number of datasets where digital polygons performed significantly better than interpolated circles (left matrix) and vice-versa (right matrix). Again the results show that digital polygons outperformed interpolated circular neighbourhoods in most cases (average value of left matrix = 5.7; average value of right matrix = 1.8). As for robustness against rotation (herein estimated through the standard deviation of the average accuracy over the angles of each dataset – last line of Tab. 3) we can see that none of the two methods clearly outperformed the other.

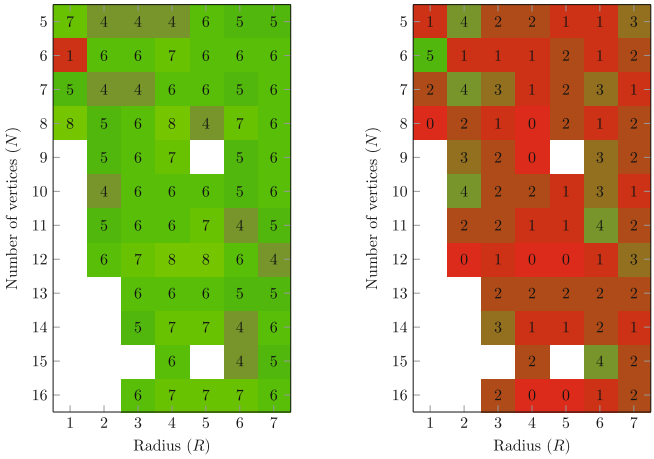

Fig. 2. Number of datasets where digital polygons performed significantly better than interpolated circles (left) and number of datasets where interpolated circles performed significantly better than digital polygons (right).

5 Conclusions and Future Work

The definition of approximately circular domains over digital images is a fundamental step for obtaining rotation-invariant texture descriptors. In this work we have proposed and investigated the use of digital polygons as a replacement for interpolated circular neighbourhoods for computing rotation-invariant features from Local Binary Patterns. Our approach employs a sub-sampling scheme over Andres' digital circles and aims at obtaining polygons with the highest circularity. The proposed method was tested on a large texture classification experiment including 69 combinations radius/number-of-pixels and eight image datasets). The results showed that LBP features computed using digital polygons were at least as accurate than those computed through interpolated circular neighbourhoods: actually, in our experiments the former outperformed the latter in most cases. As for future extensions of the present paper, we are currently working along three lines: 1) inclusion of more texture descriptors of the class Histograms of Equivalent Patterns [5] such as Improved Local Binary Patterns, Local ternary Patterns, Binary Gradient Contours, etc.; 2) extension of the analysis to multi-resolution neighbourhoods (i.e.: concentric polygons), and 3) investigation and comparison of other approaches for defining digital circles based on different neighbourhood sequences [10].

Acknowledgments. This work was supported by the Spanish Government under grant TIN2014-56919-C3-2-R and by the European Commission under project LIFE12 ENV / IT / 000411.

References

1. Andres, E., Roussillon, T.: Analytical description of digital circles. In: Debled-Rennesson, I., Domenjoud, E., Kerautret, B., Even, P. (eds.) DGCI 2011. LNCS, vol. 6607, pp. 235–246. Springer, Heidelberg (2011)
2. Bianconi, F., Fernández, A.: Rotation invariant co-occurrence features based on digital circles and discrete Fourier transform. Pattern Recognition Letters **48**, 34–41 (2014)
3. Burger, W., Burge, M.J.: Principles of Digital Image Processing: Core Algorithms. Springer (2009)
4. Fernández, A., Ghita, O., González, E., Bianconi, F., Whelan, P.F.: Evaluation of robustness against rotation of LBP, CCR and ILBP features in granite texture classification. Machine Vision and Applications **22**(6), 913–926 (2011)
5. Fernández, A., Álvarez, M.X., Bianconi, F.: Texture description through histograms of equivalent patterns. Journal of Mathematical Imaging and Vision **45**(1), 76–102 (2013)
6. González, E., Bianconi, F., Fernández, A.: General framework for rotation invariant texture classification through co-occurrence of patterns. Journal of Mathematical Imaging and Vision **50**, 300–313 (2014)
7. Klette, R., Rosenfeld, A.: Digital Geometry. Geometric Methods for Digital Picture Analysis. Morgan Kaufmann (2004)
8. Mäenpää, T., Pietikäinen, M.: Texture analysis with local binary patterns. In: Chen, C.H., Wang, P.S.P. (eds.) Handbook of Pattern Recognition and Computer Vision, 3rd edn, pp. 197–216. World Scientific Publishing (2005)
9. McIlroy, M.D.: Best approximate circles on integer grids. ACM Transactions on Graphics **2**(4), 237–263 (1983)
10. Mukherjee, J., Das, P.P., Aswatha Kumar, M., Chatterji, B.N.: On approximating Euclidean metrics by digital distances in 2D and 3D. Pattern Recognition Letters **21**(6–7), 573–582 (2000)
11. Nanni, L., Brahnam, S., Lumini, A.: Survey on LBP based texture descriptors for image classification. Expert Systems with Applications **39**(3), 3634–3641 (2012)
12. Petrou, M., García Sevilla, P.: Image Processing. Dealing with Texture. Wiley Interscience (2006)
13. Prakash, J., Rajesh, K.: A novel approach for coin identification using eigenvalues of covariance matrix, Hough transform and raster scan algorithms. World Academy of Science, Engineering and Technology **2**(8), 170–176 (2008)
14. Xie, X., Mirmehdi, M.: A galaxy of texture features. In: Mirmehdi, M., Xie, X., Suri, J. (eds.) Handbook of texture analysis, pp. 375–406. Imperial College Press (2008)